Energy Efficiency for A Plug-In Electric Vehicle with Multiple Motors and Hybrid Energy Storage System

S. Abouel-seoud[1], M. Mansy[1], M. Elshaabany[1*], M. Eltantawie[2], E. Ouda[1]
[1] Helwan University, Cairo, Egypt
[2] Higher Technological Institute, Giza, Egypt
* Corresponding Author: M. Elshaabany

ABSTRACT: *The electric vehicles gained enormous attention in the automobile industry and the research area due to the offering solutions to the vehicle's fossil fuel dependence and emissions emitted from this type of vehicle. Batteries in electric vehicles face excessive stress due to continuously charging and discharging during operation which shortens their life and inversely affects the electric vehicle's performance. The ultracapacitors (UC) are presented as a complementary energy storage device to the batteries due to their high specific power which efficiently assists in high power requirements and hill-climbing situations, as well as for energy recovery during braking. In this paper, a deterministic state machine rule-based control strategy (RBS) and fuzzy logic control strategy (FLC) for battery/ ultracapacitor hybrid energy storage system (HESS) were implemented in an electric vehicle driven by four independently in-wheel motors. The proposed control strategies were compared with passive HESS to study their effectiveness. The simulations of the electric vehicle equipped with HESS were carried out via the MATLAB/Simulink environment under the urban dynamometer driving schedule (UDDS) standard drive cycle. The simulation results showed that the RBS and FLC can fulfill the power distribution between the battery and UC however the RBS can utilize the UC energy and provide superior performance in battery energy saving than the FLC strategy.*

KEYWORDS: *Electric Vehicle, Control Strategies, Hybrid Energy Storage System, Fuzzy Logic Control*

Nomenclature

A_f	Frontal area	N_e	Number of layers of electrodes
A_i	Interfacial area between electrodes and electrolyte	N_p	Number of parallel ultracapacitors
c	Molar concentration equals $1/8N_A d^3$	N_s	Number of series ultracapacitors
C_{bat}	Battery nominal capacity	R	Ideal gas constant
C_d	drag coefficient	R_{ESR}	UC equivalent series resistance
C_T	UC module total capacitance	r_{wh}	Wheel radius
d	Molecular radius	SOC_{init}	Battery initial State f Charge
F	Faraday constant	T	Battery Operating temperature
f_r	Rolling coefficient	T_{max}	Motor maximum torque
g	Gravitational acceleration	V_{nom}	Battery nominal voltage
Gr	Total transmission ratio	V_{oc}	Single battery module voltage
J_m	Motor inertia	$\varepsilon\ \varepsilon_o$	UC permittivity of material
J_{wh}	Wheel inertia	η_{tr}	Transmission efficiency
m_v	Vehicle gross mass	ρ	Air density
N_A	Avogadro constant	N_e	Number of layers of electrodes

I. INTRODUCTION

The battery acts as the sole of the electric vehicles (EVs). It is widely used as the main energy storage device due to its characteristics for high energy density, compact size, and reliability. EVs face limited driving range due to their batteries' low specific power and power density which prevents them from performing well to meet the EVs high electric power requirements in some modes, such as high acceleration and regenerative braking. So, batteries cannot be used solely to fulfill the vehicle power demand. To improve the lifetime of the battery and meet all vehicle requirements, ultracapacitors (UCs) are widely used as a complementary source to cover the shortages of the battery and avoid undesirable battery degradation due to frequent acceleration and braking (deceleration) in EVs. UCs are characterized by high power density, a long-life cycle with high efficiency, and fast response for charging/ discharging. This fact made UCs able to meet the instantaneous high-power demand of the vehicle electric motors. It can also capture the huge energy generated during braking and assist the battery during discharge which enhances the overall vehicle performance [1]. This incorporation between high energy density source and high-power density source is called the hybrid energy storage system. The most attractive advantage deriving from HESS is the possibility of reducing the battery current stress to extend its life. One of the main obstacles in the way of a battery/ ultracapacitor hybrid energy storage system is to design a control algorithm to utilize the advantages of ultracapacitors and battery and grant good power split performance [2].

Various HESS control strategies had been designed and studied in the literature. A combined fuzzy logic control and threshold control strategy to distribute the load power demand in the HESS in sport utility vehicles at different grade roads had been studied [3]. An experimental platform had established to verify the feasibility of the fuzzy and threshold control strategies to allocate the required power between battery and ultracapacitor which the battery supplies the average power while the ultracapacitor supplies the peak power [4]. Moreover, a neural network control strategy had been implemented to predict the required power and power distribution between the battery and ultra-capacitor for battery electric vehicles. A frequency splitter technique was implemented to distribute the power demand between the battery and UC [5]. A HESS rule-based control strategy based on minimizing the fuel consumption and operating the engine at most efficient points of a parallel his hybrid electric vehicle had been implemented [6]. On the other hand, an adaptive neuro-fuzzy controller (ANFC) had been provided to control the power-sharing between the battery and ultracapacitor in battery electric vehicles. The vehicle was tested in AVL and MATLAB/Simulink environment. The proposed control strategy was compared with FLC for the same system and the simulation results showed that the ANFC can save more energy when compared with FLC over the UDDS drive cycle [7].

A dynamic programming (DP) optimal energy management system for electric vehicle HESS had designed to minimize the power loss of the battery, converters, and ultracapacitors and to study the effect of battery depth of discharge on the battery under the proposed EMS [8].Bi-level multi-objective optimal sizing and control strategy based on non-dominated sorting genetic algorithm-II and fuzzy logic control (FLC) had proposed to size the HESS and also to optimize the FLC based energy management system at the same time. [9]. FLC strategy which its rules tuned with a genetic algorithm had been implemented to manage the required power distribution between battery and ultracapacitor in an electric vehicle equipped with HESS [10].

This paper proposed two types of control strategies to control a fully active battery/ultracapacitor HESS for an electric vehicle with four independently driven in-wheel motors. A state machine rule-based control strategy and fuzzy logic control are implemented in this work to study their effectiveness. The common topologies of the HESS are briefly described in section II. Section III presents the detailed mathematical modeling of an EV combined with HESS controlled with the proposed control strategies. The hybrid energy storage system components are modeled in detail in section IV. The proposed control strategies are described in section V. Section VI presents the simulation results over the UDDS standard drive cycle. The results are demonstrated, analyzed, and compared. Finally, the work conclusion is expressed.

II. HYBRID ENERGY STORAGE SYSTEM TECHNIQUES

The battery/ultracapacitor HESS can be classified into three main topologies, each of them has its characteristics. Fig.1 shows the popular HESS configurations. In the passive topological structure Fig.1a, the battery and UC are connected parallel directly. Despite configuration simplicity, the power distribution is limited and the system has the same voltage. In the semi-active HESS, the bidirectional DC/DC converter is used to control the voltage of the UC or the battery. The battery is connected to the DC/DC converter whereas the UC is directly connected to the DC bus as shown in Fig.1b. In UC semi-active HESS as shown in Fig.1c, the UC is connected to the DC/DC converter whereas the battery is directly connected to the DC bus. In a fully active topology Fig.1d, the HESS is decoupled between battery and UC, and each source can be controlled independently

via a separate DC/DC converter. It is chosen to use the fully active topology because it is more flexible, stable, and efficient for power distribution between battery and UC. It can also reduce the weight and size of the HESS.

(a) Passive

(b) Battery Semi-Active

(c) UC Semi-Active

(d) Fully Active
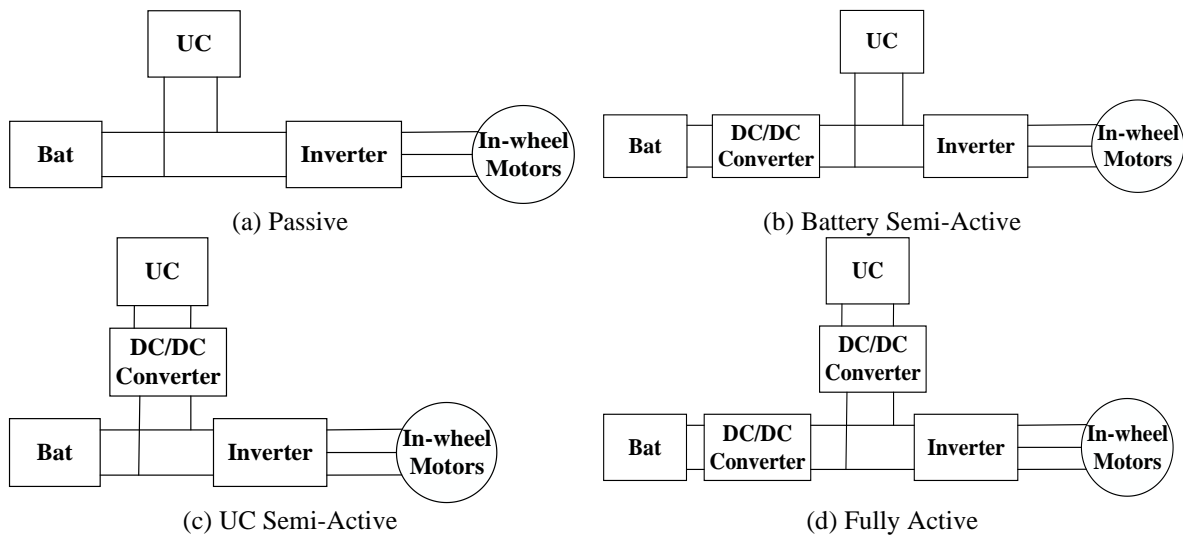
Fig.1. HESS Topologies

III. ELECTRIC VEHICLE MODELING

In this study, a forward approach model for four in-wheel motors driven electric vehicle equipped with HESS had been built in MATLAB/Simulink environment. The vehicle model consists of subsystems for vehicle longitudinal dynamics, in-wheel motors, HESS, and vehicle driver as shown in Fig.2. The power-sharing between the two energy sources has been estimated by the HESS controller. The drive cycle acts as the target vehicle speed which the driver can follow. In the vehicle driver subsystem, the vehicle actual velocity is calculated in the vehicle dynamics subsystem and compared with the speed of the drive cycle. The vehicle driver follows the drive cycle by applying the accelerator and brake pedals, which are converted into a torque request from the electric motor and the vehicle friction brake system. The in-wheel motors produce mechanical power to both the body and drive wheels. In the in-wheel motors subsystems, the required electrical power is calculated and demanded from the HESS which is controlled by the HESS controller.
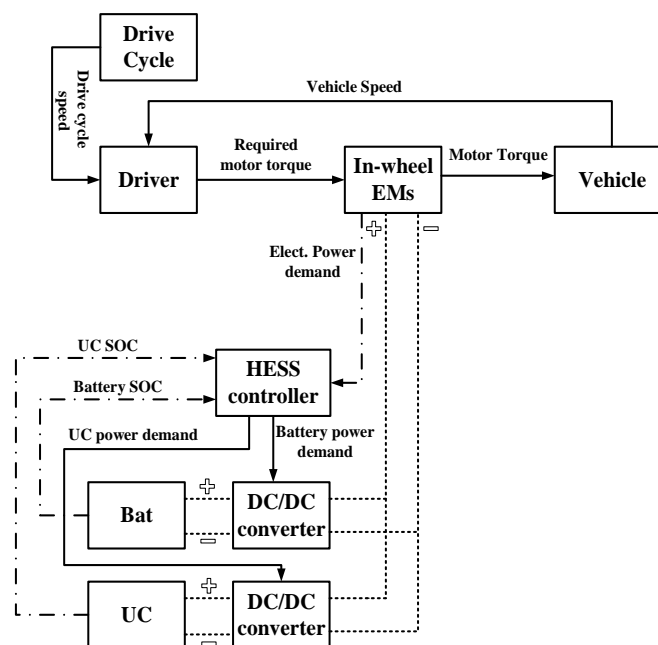
Fig.2. Electric Vehicle Model

3.1 Vehicle model

The vehicle traction force is used to overcome the various forces acting on the vehicle and propel the vehicle forward. The resistance forces at any speed are obtained by the summation of the aerodynamic drag, the rolling resistance, inertia force, and the grade resistance. It is assumed that there is no effect of the grade and wind speed on vehicle dynamics. The equations that describe the longitudinal dynamics of a road vehicle are expressed as, [11-13]:

$$V_v = 1/m_v \int (F_{tr} - mgf_r - 0.5\rho C_d A_f V_v{}^2) \tag{1}$$

$$F_{tr} = 1/r_{wh}(T_{wh} - T_{loss\_wh} - J_{wh}\, d\omega_{wh}/dt) \tag{2}$$

$$T_{wh} = (T_{mot} - T_{loss\_m} - J_m\, d\omega_{mot}/dt)G_r\eta_{tr} \tag{3}$$

$$\omega_{wh} = V_v/r_{wh} \tag{4}$$

$$\omega_{mot} = \omega_{wh}G_r \tag{5}$$

Where V_v is the vehicle speed, m_v is the gross vehicle mass, F_{tr} is the traction/braking force of the vehicle body, T_{mot} is the motor torque, T_{loss_m} is motor lost torque due to friction, T_{wh} is the drive wheel torque, $T_{loss,wh}$ is wheel lost torque due to friction and ω_{wh} is the wheel speed. Assume that there are no friction losses between the motor components and between drive wheels and hubs, so the motor and wheel lost torques can be eliminated. The vehicle dynamics model parameters are listed in Table.1.

Table.1. Vehicle dynamics model parameters, [12, 13]

Parameter	value	unit	parameter	value	unit
Vehicle gross mass (mv)	1552	kg	Total transmission ratio (Gr)	4.23	-
drag coefficient (C_d)	0.3	-	Wheel inertia (J_{wh})	4	kg*m^2
Frontal area (A_f)	1.75	m^2	Motor inertia (J_m)	0.1	kg*m^2
Rolling coefficient (f_r)	0.02	-	Wheel radius (r_{wh})	0.305	-
Gravitational acceleration (g)	9.81	m/s^2	Transmission efficiency (η_{tr})	0.95	-
Air density (ρ)	1.18	kg/m^3			

3.2 Vehicle driver model

The vehicle driver is modeled by using a classical speed feedback loop that compares the vehicle required speed from the drive cycle to the instantaneous one coming from the vehicle longitudinal dynamics subsystem. The driver model receives the drive cycle as input and depresses the accelerator or brake pedal to follow the drive cycle. The vehicle controller then calculates the torque required from the in-wheel motors and the friction brake system and the requested torques sent to the motor and power train blocks, [14]. Fig.3 shows the block diagram of the driver model.
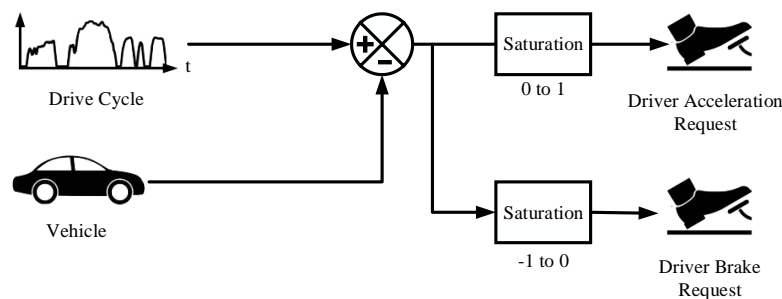
Fig.3. Driver model block diagram

3.3 In-wheel motor model

The in-wheel electric motor is a traction motor which integrated into each wheel of the proposed EV. The electric motor is the prime mover of the electric vehicle. It receives electrical power from the energy sources and supplies mechanical power for vehicle traction. During the brake mode. It operates as a generator that converts the kinetic energy stored in the vehicle body into electrical energy which recharges the energy sources. This operation is called regenerative braking. The input of the motor model is the required torque requested from the

vehicle driver. The vehicle driver requests a certain torque (T_{dem}) from the in-wheel motors according to the accelerator or brake pedal command. The motor torque can be converted to a physical signal in Simulink/Simscape environment by torque source block. The motor angular speed can be easily obtained by using a speed sensor. The output of the motor model is the required power from the HESS. The in-wheel motor model block diagram of EM modeling is shown in Fig.4.

(a) (b)
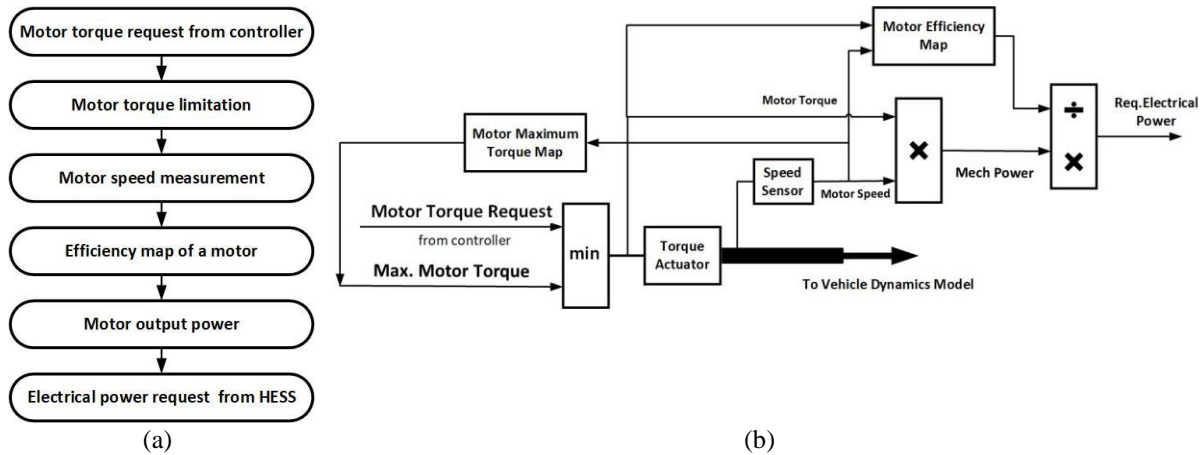
Fig.4. Flow and block diagram for the in-wheel motor modeling

The motor torque demand is limited to the motor maximum torque (T_{max})which is a function of motor speed (N_{mot}) according to the motor torque-speed characteristic curve. The motor actual torque (T_{mot}) can be estimated as, [15]:

$$T_{mot} = min(T_{dem}, T_{max}) \tag{6}$$

$$T_{max} = f(N_{mot}) \text{ where } N_{mot} = (60/2\pi)\, \omega_{mot} \tag{7}$$

Where P_{mech} is the in-wheel motor mechanical power which can be calculated as:

$$P_{mech} = T_{mot} * \omega_{mot} \tag{8}$$

The electric power demand from HESS can be estimated as:

$$P_{elect} = \begin{cases} P_{mech}/\, \eta_{mot} & \text{if } P_{mech} > 0 \; (Motoring) \\ P_{mech} * \eta_{mot} & \text{if } P_{mech} < 0 \; (Generating) \end{cases} \tag{9}$$

Based on the selected drive cycle, the required vehicle power demand is calculated. According to the power calculation, four 18kWin-wheel motors are selected as suitable traction motors. The simulation parameters of the motors are listed in Table.2. The motors are operated at the most efficient points which are selected based on its efficiency map. The in-wheel motor efficiency is a function of the motor speed and motor torque which is expressed as:

$$\eta_{mot} = f(T_{mot}, N_{mot}) \tag{10}$$

Table.2. In-wheel motor main parameters, [12]

Parameter	value	unit
Rated power	18	kw
Continuous maximum torque (T_{max})	68	N.m
Peak torque	72	N.m
Maximum speed	10000	rev/min

IV. HYBRID ENERGY STORAGE SYSTEM MODEL

The electrical power demand of the motors is requested from the HESS which combines the battery and UC. The HESS controller splits the required power between the two energy sources to benefit the advantages of each source and prolong the battery lifetime.

4.1 Battery model

The internal resistance battery model is chosen to represent theused45Ah nickel-metal hydride (Ni-MH) battery. It runs quickly and provides reasonable results. The battery model comprises a voltage source connected to a series internal resistor as shown in Fig.5.
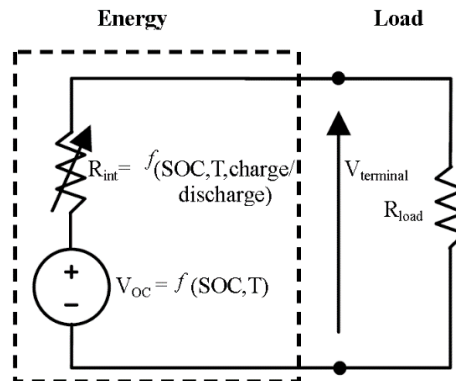
Fig.5. Battery equivalent circuit,[16]

By applying Kirchhoff's law, the terminal voltage can be calculated as,[16].

$$V_t = V_{oc} - I_{bat}R_{int} \tag{11}$$

Where V_t is the battery terminal voltage. The internal resistance (R_{int}) of each module (including interconnects) during battery charging and discharging is computed as a function of battery state of charge (SOC) and battery temperature (T). The battery SOC is used as an indicator of residual electricity of the battery and it is defined as the ratio of the charge present in the battery and the nominal charge. The open-circuit voltage of a module (V_{oc}) is also given as a function of SOC and temperature as expressed:

$$R_{int} = f(SOC, T) \tag{12}$$
$$V_{OC} = f(SOC, T) \tag{13}$$

The battery SOC can be calculated as:

$$SOC = SOC_{init} - \frac{1}{3600 * C_{bat}} \int I_{bat} \, dt \tag{14}$$

Where SOC_{init}, C_{bat}, and I_{bat} are battery initial SOC, battery nominal capacity, and battery current respectively. The battery current can be calculated as:

$$I_{bat} = V_{oc} \pm \sqrt{(V_{oc})^2 - 4 * R_{int} * P_{bat}}/(2 * R_{int}) \tag{15}$$

Where P_{bat} is the battery power demand which is a portion of the total vehicle electrical power demand which can be determined according to the power-split control strategy used in HESS. The battery voltage is estimated as, [14]:

$$V_{bat} = P_{bat}/I_{bat} \tag{16}$$

The battery pack consists of 26 modules connected in series to give a total voltage of312 volts. The main parameters of this battery are summarized in Table.3, [17].

Table.3. Battery parameters, [17]

parameter	value	unit
Single module voltage (V_{oc})	12	V
Battery nominal capacity (C_{bat})	45	Ah
Initial SOC ($SOC_{\_init}$)	100	%
Battery Temperature	25	ºC

4.2 Ultracapacitor Model

There are various models which represent the UC behavior. Among these models, the Stern-Tafel ultracapacitor model is selected to describe the double layer UC. A similar approach to the battery model is used with UC. In this case, it considers a controlled voltage source in series with an equivalent series resistance (R_{ESR}) which represents the charging and discharging resistance. The controlled voltage source is fed by the UC voltage. The UC current (I_{UC}) is estimated by using a current sensor in series with the equivalent circuit.The UC bank used in the proposed HESS composed of eight commercially available Maxwell BMOD0165 P048modules.There are some considerations taken during UC modeling as the total capacitance and equivalent series resistance remains constant during simulation, the model is temperature independent and the current passing through the supercapacitor is continuous, [18].The model parameters of the ultracapacitor bank are listed in Table.4. Fig.6 shows the equivalent circuit of the UC. The UC voltage (V_{UC})and total electric charge (Q_t)can be evaluated as, [19, 20]:

$$V_{UC} = V_{tot} - R_{ESR}I_{UC} \tag{17}$$

$$V_{tot} = \frac{N_s Q_t d}{N_p N_e \varepsilon\varepsilon_o A_i} + \frac{2N_e N_s RT}{F}\sinh^{-1}\left(\frac{Q_t}{N_p N_e{}^2 A_i\sqrt{8RT\varepsilon\varepsilon_o c}}\right) \tag{18}$$

$$Q_t = \int_0^t I_{UC}dt \tag{19}$$

Where t is the period of the drive cycle. The ultracapacitor SOC can be estimated as, [17]:

$$SOC_{UC} = \frac{1}{Q_{max}}\left(Q_{int} - \int_0^t I_{UC}dt\right) \tag{20}$$

Where V_{tot}, I_{UC}, Q_{max}, and Q_{int} are the total UC voltage, UC current, the maximum and initial UC electric charges respectively. The UC is fully charged; therefore, the initial UC charge is set to the maximum UC electric charge. The maximum UC electric charge can be evaluated as:

$$Q_{max} = C_T * V_{nom} \tag{21}$$
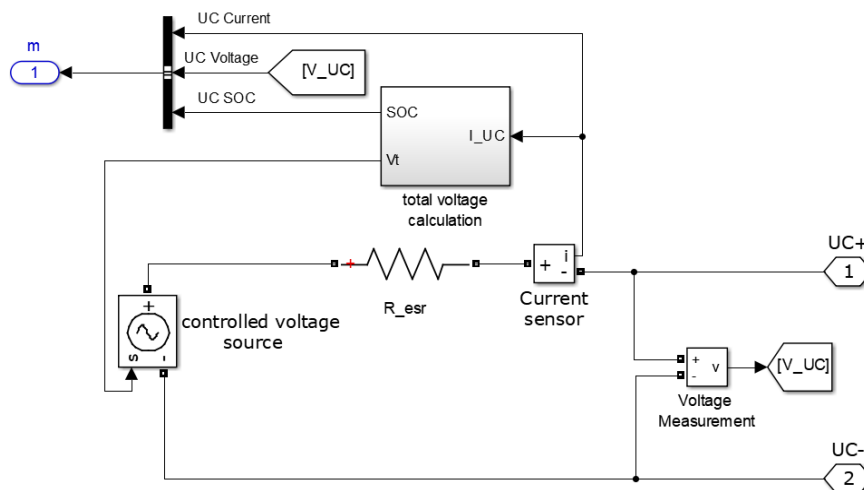
Fig.6. Ultracapacitor equivalent circuit

Table.4. Ultracapacitor model parameters, [17]

parameter	Value	unit
Nominal Voltage (V_{nom})	388	V
Module total capacitance (C_T)	165	F
Equivalent series resistance (R_{ESR})	50.4	mΩ
Interfacial area between electrodes and electrolyte (A_i)	3731	m^2
Molar concentration (c)	207.57	mol/m^3
Faraday constant(F)	$9.648*10^4$	C/mol
Number of layers of electrodes (N_e)	1	-
Avogadro constant (N_A)	6.022×10^{23}	Mol^{-1}
Number of parallel supercapacitors (N_p)	1	-

Number of series supercapacitors (N_s)	144	-
Ideal gas constant (R)	8.314	J/mol.K
Molecular radius (d)	$1*10^{-9}$	m
Operating temperature (T)	300	K
Permittivity of material ($\varepsilon\ \varepsilon_o$)	6.0208×10^{-10}	F/m

4.3 DC/DC converter

A fully active HESS employed in this study uses two bidirectional DC/DC converters to make the power flow between the battery and UC controllable. From the power balance principle, the total power demand from the motors equals the power requested from the energy storage system (ESS) i.e. battery or UC or both. The requested electrical power and current from ESS can be estimated as,[21]:

$$P_{ESS} = P_{DC} + P_{loss} = I_{DC}V_{DC} + I_{DC}{}^2 R_{loss}) \tag{22}$$

$$I_{ESS} = \frac{(P_{DC} + P_{loss})}{V_{ESS}} \tag{23}$$

Where P_{ESS} is the power required from the ESS, P_{DC} is DC bus power, P_{loss} represents the DC/DC converter losses which simulated by a resistor (R_{loss}), I_{ESS} is the ESS current, V_{ESS} is the ESS voltage, V_{DC} is DC bus voltage and I_{DC} is the DC bus current. The simplified DC/DC converter model is shown in Fig.7. According to an algorithmic procedure, the HESS controller calculates the power required from each energy source so at any time, the sum of the required powers, $P_{bat,req}$ and $P_{uc,req}$ should be identical to the electric power demand to supply the electric motors as:

$$P_{elect} = P_{bat,req} + P_{uc,req} \tag{24}$$
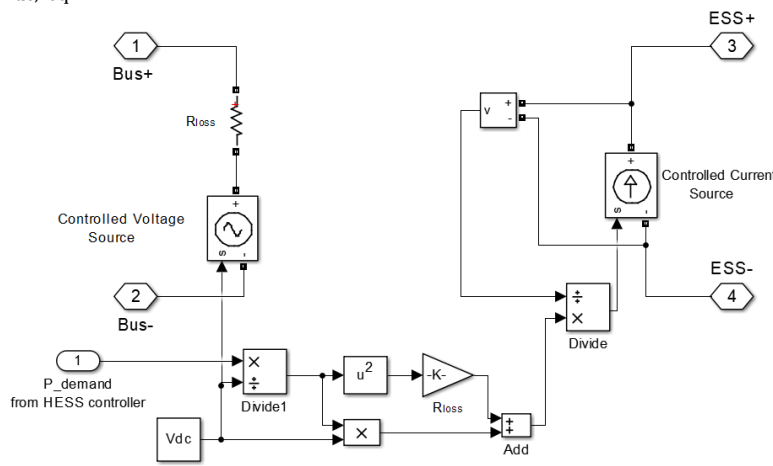
Fig.7. DC/DC converter model

V. HYBRID ENERGY STORAGE SYSTEM CONTROL

The objective of the HESS controller is to determine the ideal distribution of the power demand between the two energy sources in a manner that save the battery and prolong its lifetime. In this work, two HESS control strategies are implemented. The first is the state machine rule-based control and the second is the fuzzy HESS control.

5.1 Rule-Based HESS control

In this section, a state machine rule-based control strategy for HESS had been proposed. This strategy is one of the deterministic rule-based control strategies. The main concept of this control strategy is that at high load requirements, most demand power is supplied by the UC bank and the rest by the battery. The battery provides electric power at average vehicle load (P_{avg}) to extend the battery life. During regenerative brake, most power provided from the motor is recovered by UC, and the remaining power is recovered by the battery. The proposed state machine rule-based control strategy is designed and established in MATLAB/Stateflow environment as shown in Fig.8. To save the HESS components and ensure adequate operation of these components, some constraints are necessary should be considered as:

$$SOC_{UC\_max} > SOC_{UC} > SOC_{UC\_min}$$
$$SOC_{bat\_max} > SOC_{bat} > SOC_{bat\_min}$$

(25)

Where SOC_{UC_max}, SOC_{UC_min}, SOC_{bat_max}, and SOC_{bat_min} are ultracapacitor maximum SOC, ultracapacitor minimum SOC, battery maximum SOC and battery SOC respectively. The battery SOC is limited between 20% and 100% whereas the ultracapacitor SOC is set between 25% and 90%,[22]. It is assumed that the initial SOC for the battery and ultracapacitor are 100%.
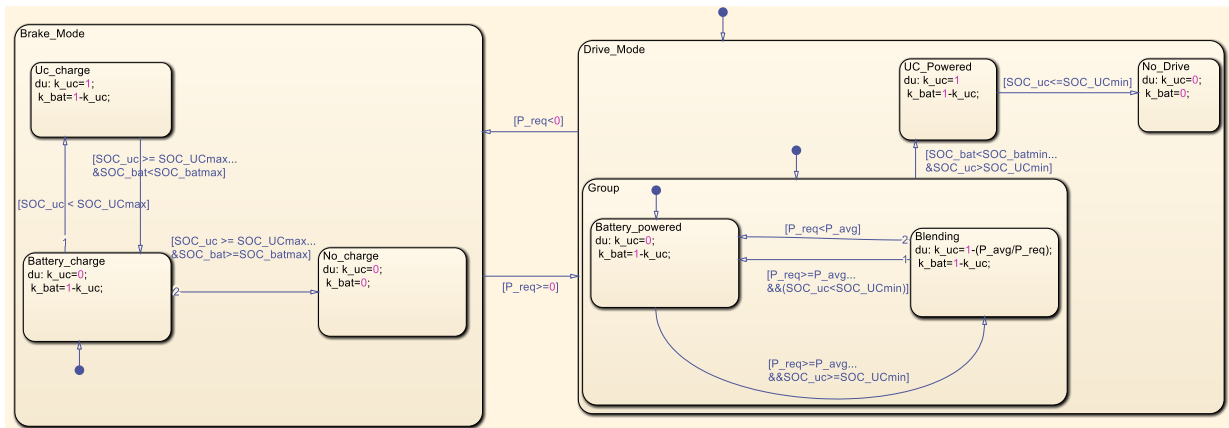
Fig.8. Rule-based control strategy

5.2 Fuzzy HESS Control

FLC is an effective control strategy that is commonly used in energy management systems for EVs due to its convenience. It converts the crisp inputs into linguistic variables that humans use in their everyday lives to base sensitive decisions and apply general rules based on experience that should be applied to those control situations which demand them. The gained knowledge can be a great tool to reduce the undesired effects of the system response. A Mamdani type FLC is proposed in this work to split the demand power between the battery and UC. The proposed FLC strategy includes three input variables that directly affect the HESS performance which are battery SOC (SOC_B), ultracapacitors SOC (SOC_{UC}), and demand power from the HESS (P_{req}) which represented here as a ratio of the demand power to the maximum power. The output of the proposed FLC is the UC power split ratio (k_{UC}) which is the ratio between the UC demand power to the total demand power. Therefore, the demand power of the battery can be easily calculated. The proposed FLC rule base includes 84 rules. The proposed FLC strategy configuration and fuzzy membership functions are shown in Fig.9 and Fig.10 respectively. Fig.11 shows the response surface of the proposed FLC which represents the HESS inputs/output relationship. The change of the FLC output k_{UC} with the battery SOC and ultracapacitor SOC is shown in Fig.11a. The change of the FLC output k_{UC} with ultracapacitor SOC and demand power is presented in Fig.11b. Finally, the change of k_{UC} with the battery SOC and demand power is shown in Fig.11c.
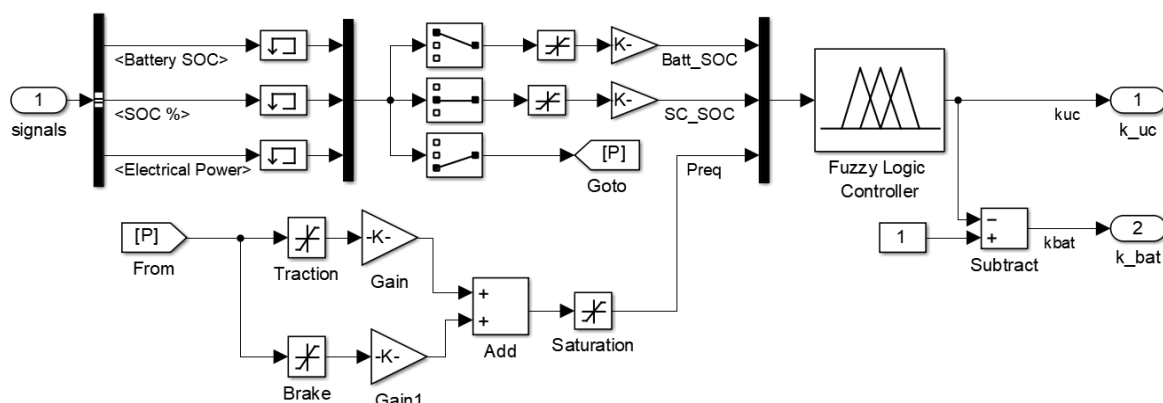
Fig.9. proposed HESS fuzzy logic control strategy

(a)

(b)

(c)

(d)
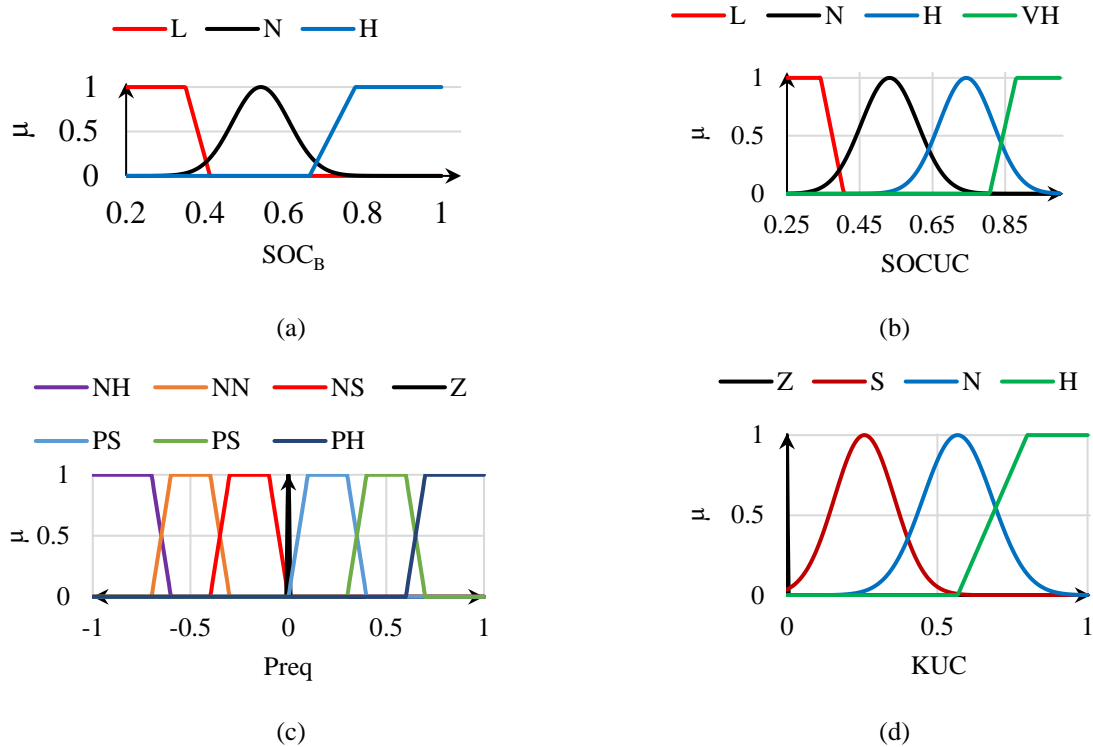
Fig.10. Fuzzy membership functions (a) Input variable SOC_b, (b) Input variable SOC_{UC}, (c) Input variable P_{req}, (d) Output variable K_{UC}

(a)

(b)

(c)
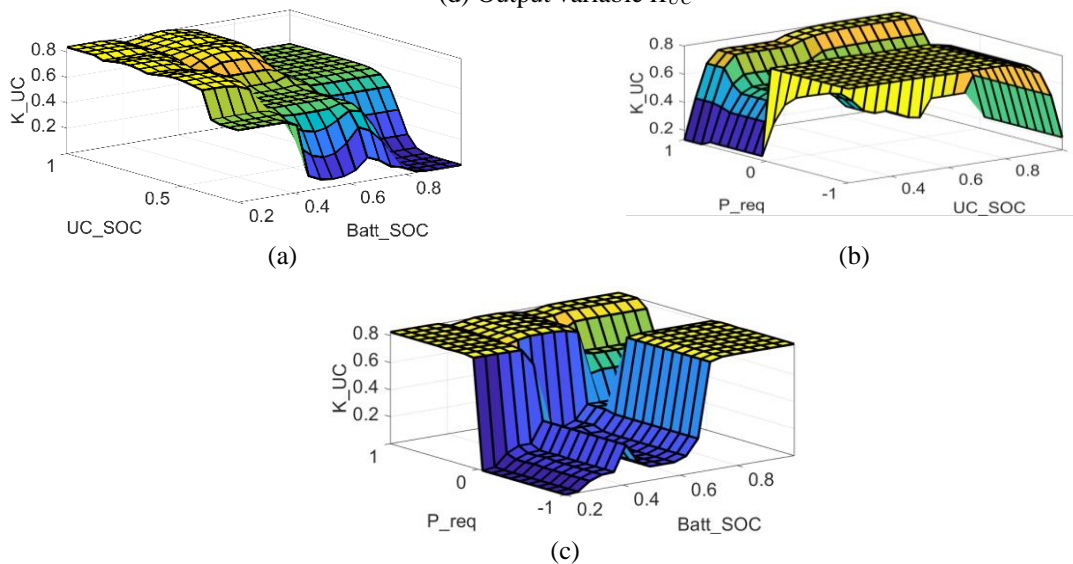
Fig.11. FLC surface output K_{UC} concerning (a) battery SOC and ultracapacitor SOC, (b) ultracapacitor SOC and demand power (c) battery SOC and demand power

VI. RESULTS AND DISCUSSION

In this section, the results of the proposed HESS control strategies are presented, analyzed, and compared with passive HESS. The EV model has been built and simulated using the MATLAB/Simulink environment under UDDS standard urban drive cycle to examine the power flow in HESS and show the effectiveness of the proposed HESS control strategies. The UDDS drive cycle is shown in Fig.12 and it is chosen due to its frequent stop and start which can exhibit the charging/discharging performance of the battery and UC. The drive cycle data was

obtained from the United States Environmental Protection Agency (EPA) [23]. The root mean square values of the grouped data is used as a comparison index of the performance of the proposed HESS control strategies.
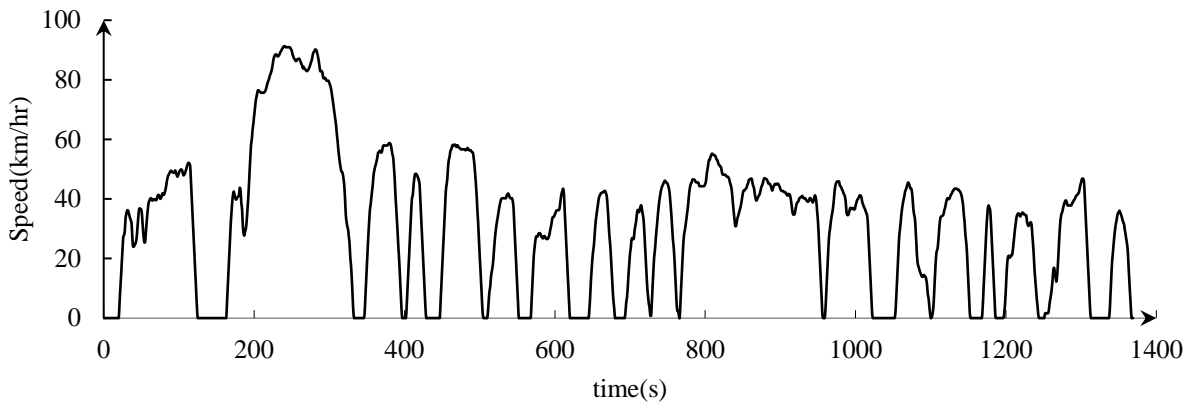
Fig.12. UDDS drive cycle

Fig.13 shows the battery SOC comparison between the proposed control strategies, passive HESS, and when the battery is used as a single source. As seen, it is noticed that there are several differences between the magnitudes of the SOC along the drive cycle however the trends of the SOC curves of passive HESS, HESS controlled by RBS, and FLC always have a higher value than the battery stand-alone curve. This indicates that the existence of the UC in EV alleviates the encumbrance on the battery. As shown in the zoomed interval, the battery SOC at the end of the drive cycle of battery only, passive HESS, HESS controlled by RBS, and FLC are declined by 12.51%,10.22%,10.166%, and 10.37% respectively. The RBS had the highest value of the SOC almost the drive cycle which leads to decrease the stress on the battery and save more energy. This energy can be reused later in other applications.
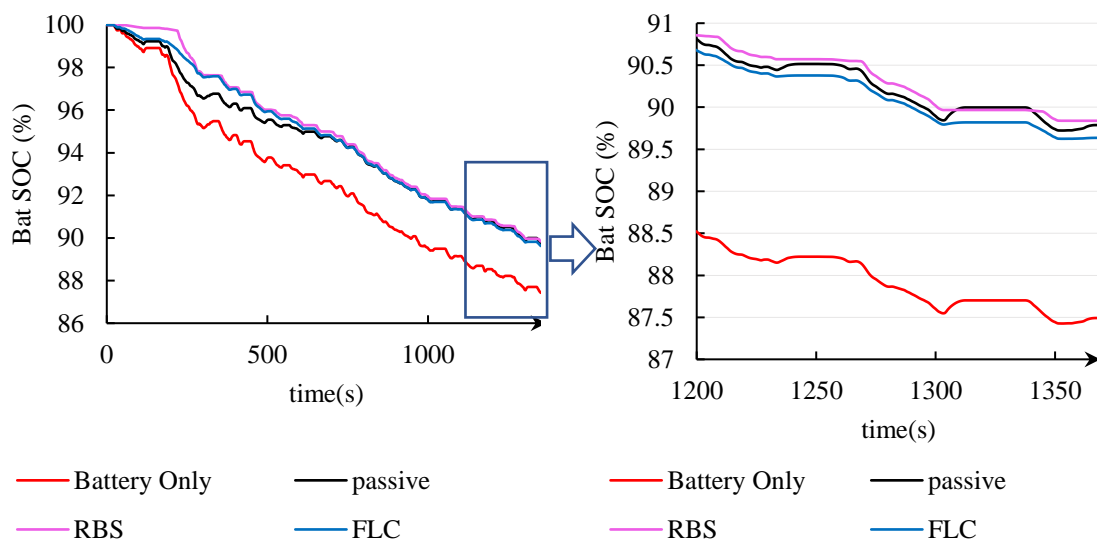
Fig.13. Battery SOC

The ultracapacitor SOC history over the drive cycle is shown in Fig.14. it is noticed that in passive HESS, the UC is fully depleted nearly at the mid-range of the drive cycle which means that the vehicle will be propelled the rest of the drive cycle with the battery only. In the RBS control strategy, it is noticed that when the UC SOC depleted to its minimum allowable value (25%), the controller stops feeding the vehicle loads with UC energy and the battery feeds solely the vehicle load till the UC can be recharged again with regenerative braking energy and be able to propel the vehicle. The FLC strategy utilized the UC well at the beginning of the drive cycle compared with passive HESS but holds and captures more energy than the RBS strategy at the rest of the drive

cycle which indicates that the FLC strategy is not capable of using the UC energy at the best way and this acts as a drawback of this proposed strategy.
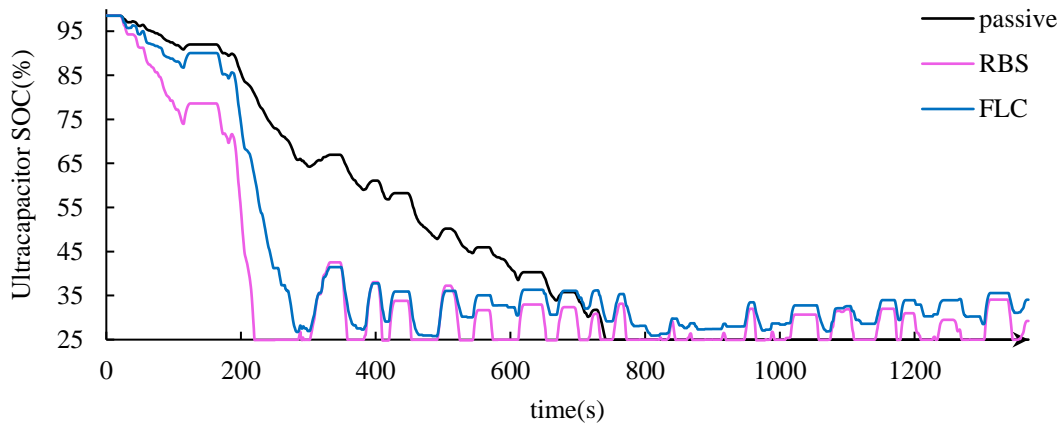
Fig.14. Ultracapacitor SOC

Fig.15 illustrates the battery power at different control strategies during the interval from 200 to 400 seconds of the drive cycle. It is observed that all curves have different values according to the implemented control strategy in the positive Y-axis which indicates that the discharging power in the motoring mode of the motor. However, in the negative Y-axis which indicates the battery charging power during regenerative braking mode. It is shown that charging and discharging power is very high when the battery is used as a single source compared to the proposed HESS strategies. The passive HESS records the highest value of charge power as the charge power generated during braking mode can be recycled by UC instead of the battery according to the applied control strategy. In the RBS strategy, when the UC is depleted as shown in the period from 220 to 290 seconds, the UC power curve follows the UC power curve of battery only case. In this case, the battery supplies exclusively the vehicle load. It is shown also that when the vehicle in the regenerative braking mode. The battery doesn't recycle the regenerative braking energy as the UC absorbs this energy instead of the battery. When the required power is high, the battery covers only the average required power, and the remaining power is covered by the UC. As shown in Fig.21, the lowest discharge power is achieved when RBS is applied compared with FLC.
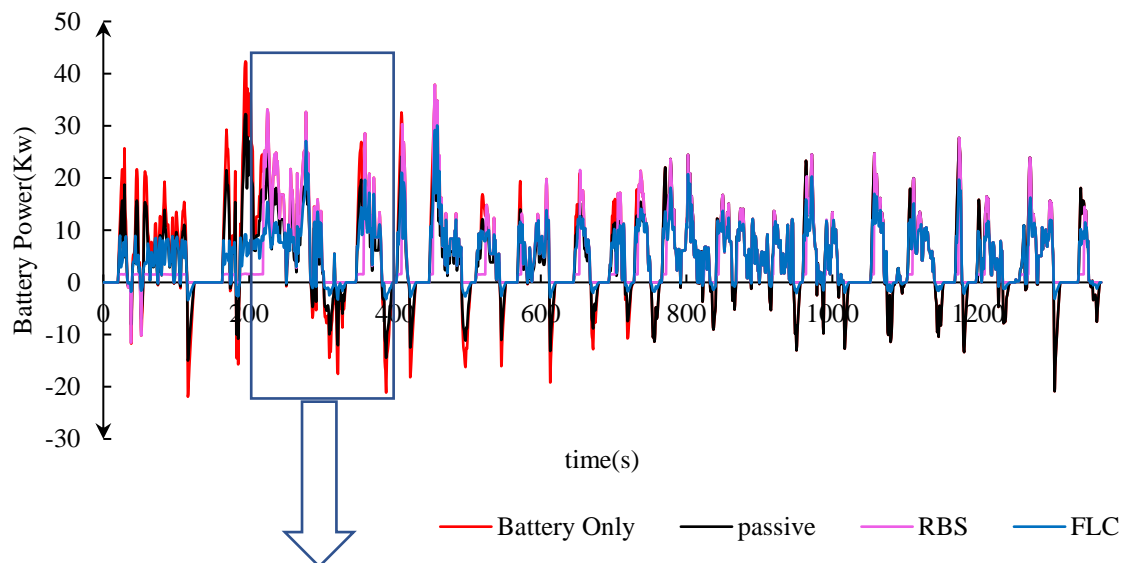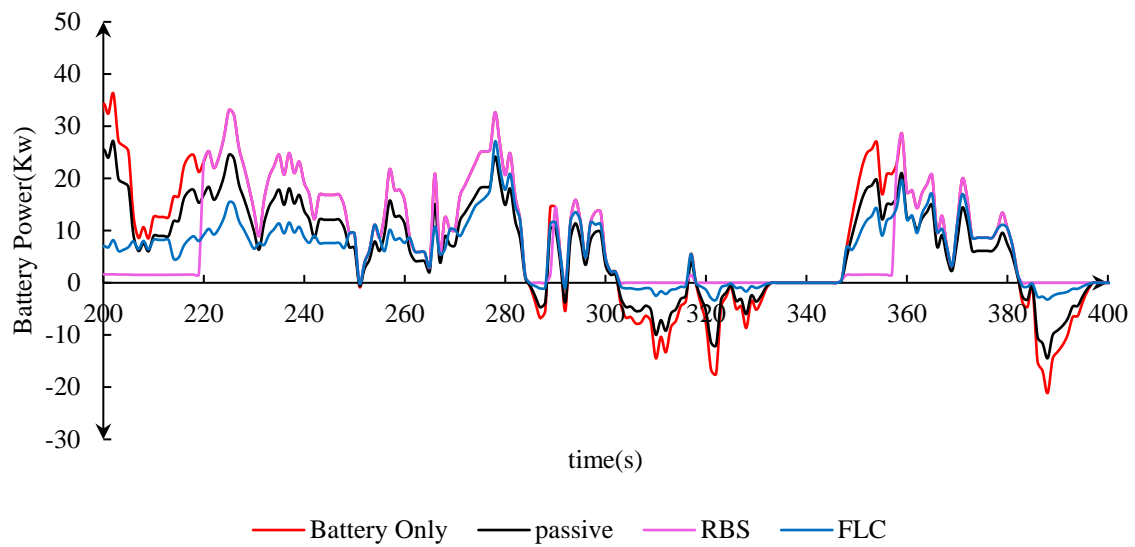
Fig.15. Battery power

The UC power history between 200 to 400 seconds of the drive cycle is shown in Fig.16. When RBS strategy was applied, it was noticed that at the period between 220 to 290 seconds, UC is fully depleted in RBS strategy and the UC power decreased to zero this allows the battery to feeds the vehicle loads solely. Otherwise, it is noticed that the RBS control strategy achieved the highest UC discharge power during vehicle traction and it also achieved the greatest regenerated power during braking.
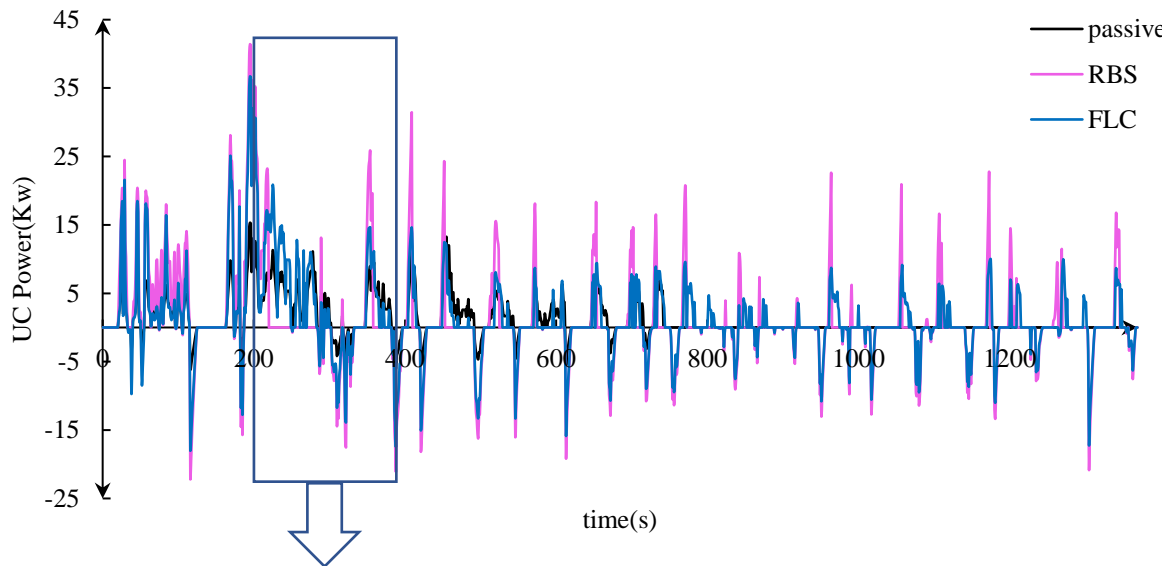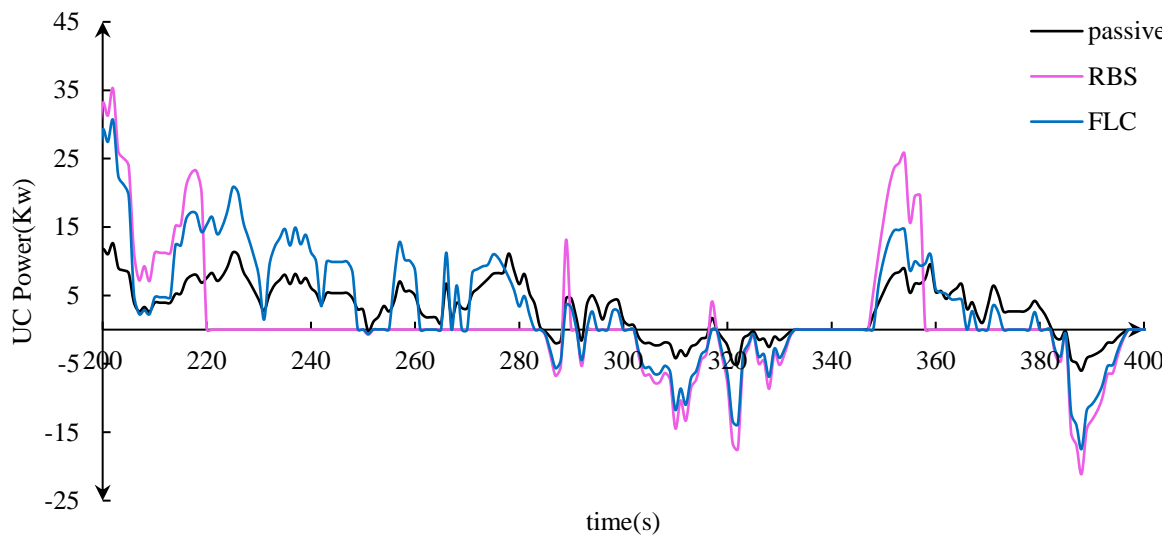
Fig.16.UC power

The battery discharge energy is presented in Fig.17. It is clear that the maximum energy is consumed during traction when the battery is used as a single source however the minimum energy is obtained when the RBS control strategy is applied. The battery discharging energy decreased by 6.53% when the RBS strategy is applied compared with the FLC strategy.
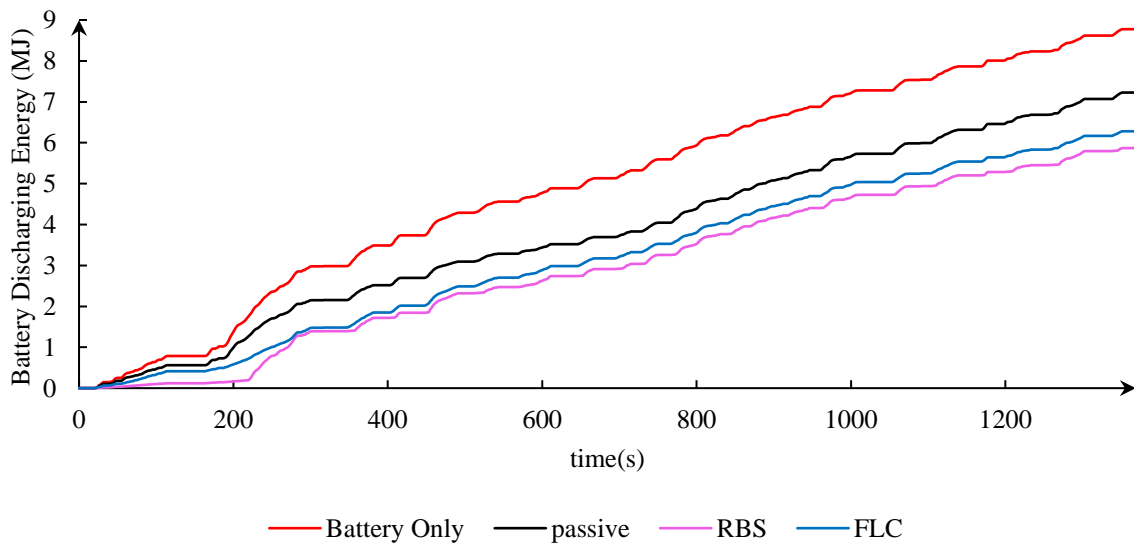
Fig.17. Battery traction energy

The battery charging energy is presented in Fig.18. The highest value of the regenerated energy can be obtained when the battery is solely used however the minimum value is obtained when the RBS strategy is used. The battery charging energy decreased by 87.1% when the RBS strategy is applied compared with the FLC strategy.
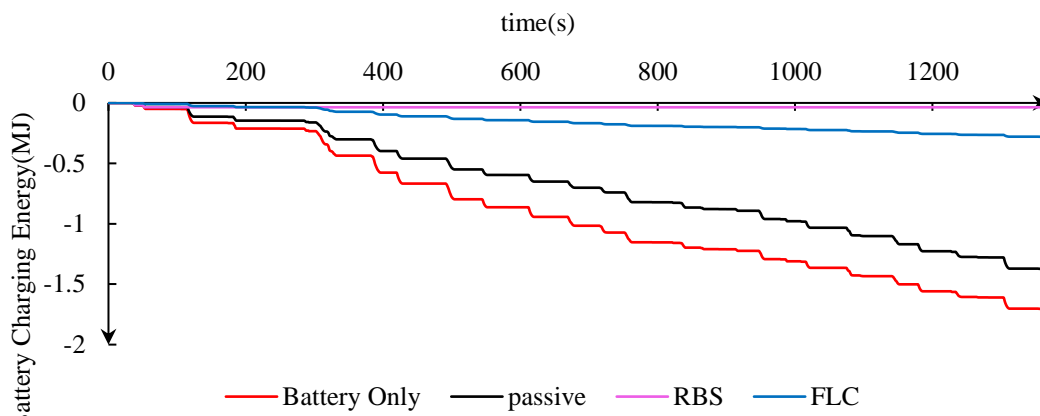
Fig.18. Battery regenerated energy

The RBS control strategy offers the best exploitation of the UC energy whether in traction mode or in regenerative braking mode as shown in Figs19,20. In the vehicle traction mode, the results show that the UC discharge energy increased by 7.98% when the RBS strategy is applied compared to the FLC strategy. In regenerative braking mode, the UC charge energy increased by 18.18% when the RBS strategy is applied compared with the FLC strategy.
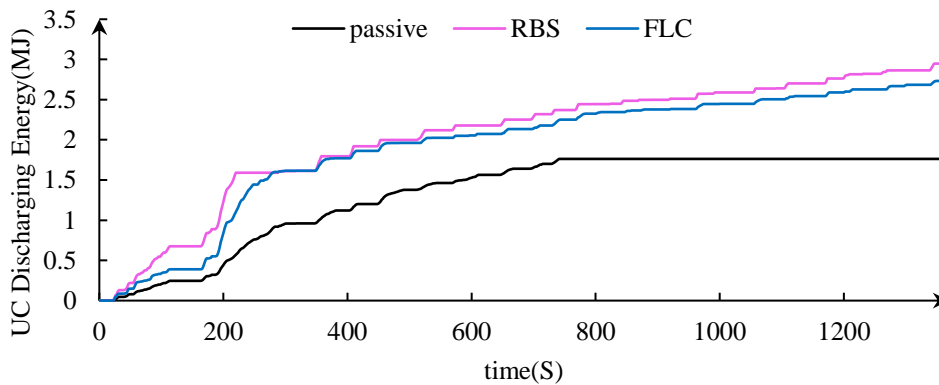
Fig.19.UC traction energy
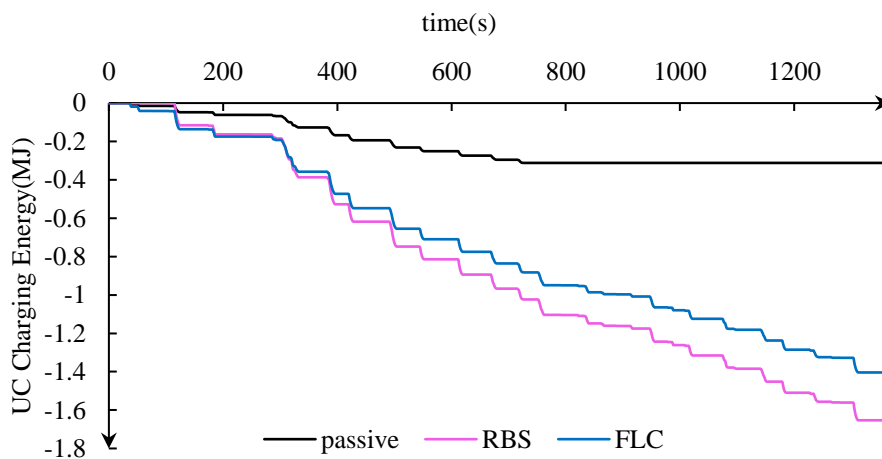
Fig.20.UC regenerated energy

The charts in Fig.21 present the comparisons between the mean value of the performance parameters after applying the proposed control strategies. The improvement of HESS controlled with RBS and FLC strategies

compared with passive HESS is presented in Table 5. The improvements are estimated as a percentage and the up arrow illustrates the value increment whereas the down arrow illustrates the value reduction.
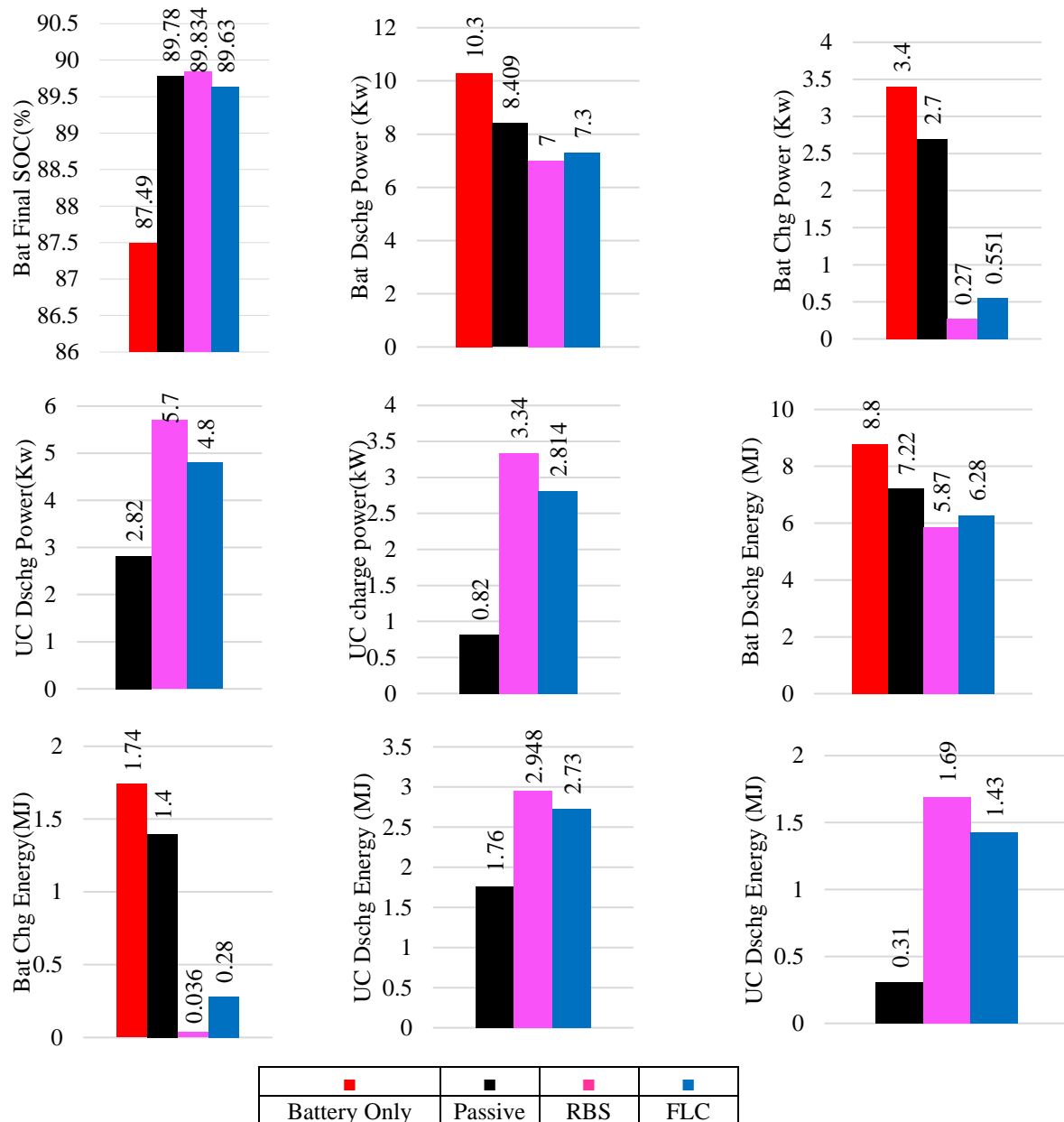
Fig.21. Comparison between the proposed control strategies, passive HESS, and battery only scenarios over the UDDS drive cycle

Table 5. Improvement of HESS controlled with RBS and FLC strategies compared with passive HESS

Performance Parameter	RBS	FLC	Performance Parameter	RBS	FLC
Battery SOC (%)	↑0.06	↓0.16	Battery discharge Energy (%)	↓18.7	↓13
Battery discharge power (%)	↓16.75	↓13.19	Battery charge Energy (%)	↓97.43	↓80
Battery charge power (%)	↓90	↓79.6	UC discharge Energy (%)	↑67.5	↑55.11
UC discharge power (%)	↑102.12	↑70.21	UC charge Energy (%)	↑445.2	↑361.3
UC charge power (%)	↑307.31	↑243.2			

VI. CONCLUSION

The EV battery faces high stress due to frequent charging and discharging cycles during vehicle operation which shortens its life. The battery isn't an ideal energy storage system especially in regenerative braking mode as it could not absorb all the energy generated during braking. A secondary energy storage system can be supplemented to the EV to supply the vehicle required power in certain situations. This combination eliminates the shortcomings of the battery. Battery/ultracapacitor energy storage system hybridization of the EVs showed a great impact on battery life improvement and vehicle performance. In this paper, two HESS control strategies had been implemented: The first control strategy is a deterministic state machine rule-based control strategy that finds the optimal power distribution between the battery and UC based on a set of states. The second control strategy is Mamdani type FLC using the EV demand power from the HESS and the state of charge of the battery and UC as inputs and power ratio of the UC power to the total demand power as output. The proposed control strategies are compared with fixed ratio passive HESS to show the effectiveness of the proposed strategies. The HESS is established and simulated via MATLAB/Simulink software and the simulation results proved that the HESS control strategies can save the energy of the battery effectively compared with when the battery is used solely. The results showed that the FLC strategy reduced the battery discharge energy by 13% compared with the passive HESS. This reduces the stress in the battery and increases the life of the battery. The UC discharge energy increased by 55.11% when the FLC is applied compared with passive HESS and the UC regenerative braking energy also increased by 361.3% compared with the passive HESS. Although the huge improvements of the FLC, it is found that the RBS control strategy offered a great performance compared with the FLC control strategy. The battery discharge energy decreased by 18.7% compared with the passive HESS while the battery charge energy increased by 97.5%. the UC discharge energy increased by 67.5% when applying the RBS compared with the passive HESS while the UC charge energy increased by 445.2% when applying the RBS compared with the passive topology. The results showed that the RBS effectively decreases the battery discharge energy, prolongs the battery service life, and utilizes the advantages of the UC which reduces the battery stress and energy consumption and as a result increases the vehicle mileage.

REFERENCES

[1]. C. Zhang, D. Wang, B. Wang, and F. Tong, "Battery Degradation Minimization-Oriented Hybrid Energy Storage System for Electric Vehicles", Energies, vol. 13, pp. 246, 2020.

[2]. Q. Zhang, and G. J. E. E. Li, "A predictive energy management system for hybrid energy storage systems in electric vehicles", Electrical Engineering, Springer, vol. 101, no. 3, pp. 759-770, 2019.

[3]. T. Dhia, N. A. Mardiyah, and N. Nurhadi, "Fuzzy Logic Control Design in Hybrid Energy Storage System Super-Capacitor Battery for Electric Vehicle", Kinetik: Game Technology, Information System, Computer Network, Computing, Electronics, and Control, pp. 75-86, 2018.

[4]. M. Zhou, Z. Liu, and J. Feng, "Research on the energy management of composite energy storage system in electric vehicles", International Journal of Electric and Hybrid Vehicles, vol. 10, no. 1, pp. 41-56, 2018.

[5]. Q. Zhang, W. Deng, and G. Li, "Stochastic Control of Predictive Power Management for Battery/Supercapacitor Hybrid Energy Storage Systems of Electric Vehicles", IEEE Transactions on Industrial Informatics, vol. 14, no. 7, pp. 3023-3030, 2018.

[6]. A. H. Eghbali, B. Asaei, and P. Nader, "Fuel efficient control strategy, based on battery-ultracapacitor energy storage system, in parallel hybrid electric vehicles", 2010 IEEE Vehicle Power and Propulsion Conference, pp. 1-5, 2010.

[7]. E. H. K. Fung, Y. Wang, and Y. K. Wong, "Adaptive Neural-Fuzzy Controller (ANFC) Based Energy Management System for Battery/Ultracapacitor Electric Vehicle", ASME 2012 International Mechanical Engineering Congress and Exposition, pp. 283-289, 2012.

[8]. J. Liu, H. Dong, T. Jin, L. Liu, B. Manouchehrinia, and Z. Dong, "Optimization of Hybrid Energy Storage Systems for Vehicles with Dynamic On-Off Power Loads Using a Nested Formulation", Energies, vol. 11, no. 10, pp. 2699, 2018.

[9]. L. Zhang, X. Hu, Z. Wang, F. Sun, J. Deng, and D. G. Dorrell, "Multiobjective Optimal Sizing of Hybrid Energy Storage System for Electric Vehicles", IEEE Transactions on Vehicular Technology, vol. 67, no. 2, pp. 1027-1035, 2018.

[10]. J. Javorski Eckert, L. Corrêa de Alkmin e Silva, F. Mazzariol Santicciolli, E. dos Santos Costa, F. C. Corrêa, and F. Giuseppe Dedini, "Energy storage and control optimization for an electric vehicle", International Journal of Energy Research, vol. 42, no. 11, pp. 3506-3523, 2018.

[11]. M. Choi, J. Lee, and S. Seo, "Real-Time Optimization for Power Management Systems of a Battery/Supercapacitor Hybrid Energy Storage System in Electric Vehicles", IEEE Transactions on Vehicular Technology, vol. 63, no. 8, pp. 3600-3611, 2014.

[12]. F. Odeim, J. Roes, L. Wülbeck, and A. Heinzel, "Power management optimization of fuel cell/battery hybrid vehicles with experimental validation", Journal of Power Sources, vol. 252, pp. 333-343, 2014.

[13]. V. I. Herrera, A. Saez-de-Ibarra, A. Milo, H. Gaztañaga, and H. Camblong, "Optimal energy management of a hybrid electric bus with a battery-supercapacitor storage system using genetic algorithm", 2015 International Conference on Electrical Systems for Aircraft, Railway, Ship Propulsion and Road Vehicles (ESARS), pp. 1-6, 2015.

[14]. W. Liu, "Hybrid Electric Vehicle System Modeling",in Hybrid Electric Vehicle System Modeling and Control, pp. 38-96, Wiley, 2017.

[15]. J.-y. Liang, J.-l. Zhang, X. Zhang, S.-f. Yuan, and C.-l. Yin, "Energy management strategy for a parallel hybrid electric vehicle equipped with a battery/ultra-capacitor hybrid energy storage system", Journal of Zhejiang University SCIENCE A, vol. 14, no. 8, pp. 535-553, 2013.

[16].   A. Jarushi, and N. Schofield, "Modelling and Analysis of Energy Source Combinations for Electric Vehicles", World Electric Vehicle Journal, vol. 3, no. 4, 2009.

[17].   S. S. Williamson, "Hybrid Electric and Fuel Cell Hybrid Electric Vehicles",in Energy Management Strategies for Electric and Plug-in Hybrid Electric Vehicles, pp. 31-63, New York, NY, Springer New York, 2013.

[18].   V. Tejwani, and B. Suthar, "Energy Management System in Fuel Cell, Ultracapacitor, Battery Hybrid Energy Storage", International Journal of Electronics Communication Engineering, vol. 9, no. 12, pp. 1492-1500, 2016.

[19].   K. B. Oldham, "A Gouy–Chapman–Stern model of the double layer at a (metal)/(ionic liquid) interface", Journal of Electroanalytical Chemistry, vol. 613, no. 2, pp. 131-138, 2008.

[20].   H. Miniguano, A. Barrado, C. Fernández, P. Zumel, and A. Lázaro, "A General Parameter Identification Procedure Used for the Comparative Study of Supercapacitors Models", Energies, vol. 12, no. 9, pp. 1776, 2019.

[21].   S. K. Kollimalla, and M. K. Mishra, "Analysis and control of DC-DC boost converter using average power balance control (APBC)", 2012 4th International Conference on Intelligent and Advanced Systems (ICIAS2012), pp. 513-518, 2012.

[22].   S. Zhang, R. Xiong, and F. Sun, "Model predictive control for power management in a plug-in hybrid electric vehicle with a hybrid energy storage system", Applied Energy, vol. 185, pp. 1654-1662, 2017.

[23].   United States Environmental Protection Agency (EPA), "urban dynamometer driving schedule (UDDS)," [Online]. Available: https://www.epa.gov/sites/production/files/2015-10/uddscol.txt, [Accessed: 20 March 2020].